

Rhodopsin Transport in the Membrane of the Connecting Cilium of Mammalian Photoreceptor Cells

Uwe Wolfrum* and Angelika Schmitt

Institute of Zoology, Johannes Gutenberg-University of Mainz, Mainz, Germany

The transport of the photopigment rhodopsin from the inner segment to the photosensitive outer segment of vertebrate photoreceptor cells has been one of the main remaining mysteries in photoreceptor cell biology. Because of the lack of any direct evidence for the pathway through the photoreceptor cilium, alternative extracellular pathways have been proposed. Our primary aim in the present study was to resolve rhodopsin trafficking from the inner to the outer segment. We demonstrate, predominantly by high-sensitive immunoelectron microscopy, that rhodopsin is also densely packed in the membrane of the photoreceptor connecting cilium. Present prominent labeling of rhodopsin in the ciliary membrane provides the first striking evidence that rhodopsin is translocated from the inner segment to the outer segment of wild type photoreceptors via the ciliary membrane. At the ciliary membrane rhodopsin co-localizes with the unconventional myosin VIIa, the product of human Usher syndrome 1B gene. Furthermore, axonemal actin was identified in the photoreceptor cilium, which is spatially co-localized with myosin VIIa and opsin. This actin cytoskeleton of the cilium may provide the structural bases for myosin VIIa-linked ciliary trafficking of membrane components, including rhodopsin. *Cell Motil. Cytoskeleton* 46:95–107, 2000. © 2000 Wiley-Liss, Inc.

Key words: photoreceptor; rhodopsin; cilium; myosin; actin; Usher Syndrome; ciliary transport

INTRODUCTION

Vertebrate photoreceptor cells are highly specialized and polarized neurons, divided into several morphologically and functionally distinct compartments (Fig. 1a): the photoreceptor outer segment and inner segment continuing into the perikaryon and the synaptic region, where the electrical signal generated in the photoreceptor cell is transmitted to other neurons of the neuronal retina. The two segments of photoreceptor cells are linked by a thin cellular bridge, the modified nonmotile connecting cilium. Photoreceptor outer segments contain hundreds of flattened membrane disks bearing all components of the visual transduction cascade. The phototransductive membranes of the outer segment are continually renewed throughout the lifetime of the individual. Newly synthesized membrane is added at the base of the outer segment by the expansion of the plasma membrane [Steinberg et al., 1980] or by incorporation of vesicular structures into nascent disk membranes [Usukura and Obata, 1995], whereas disks at the distal tip of the outer segment are

phagocytized by the cells of the retinal pigment epithelium [Young, 1976].

However, rhodopsin, the most prominent membrane protein of outer segment membranes (~85% of total outer segment protein) [Hall et al., 1969; Corless et al., 1976], is synthesized at the rough endoplasmic reticulum in the proximal inner segment and therefore, a large number of newly synthesized rhodopsin molecules (~ 10^7 molecules/day per cell) must be transported to the base of the outer segments. Immunocytochemical studies conducted by Papermaster et al. [1985, 1986] indicate

Grant sponsor: Deutsche Forschungs Gemeinschaft, Grant number: Wo 548/3; Grant sponsor: Forschung Contra Blindheit-Initiative Usher Syndrom e.V.; Grant sponsor: FAUN-Stiftung, Nürnberg, Germany.

*Correspondence to: Uwe Wolfrum, Institute of Zoology, Department 1, Johannes Gutenberg-University of Mainz, Müllerweg 6, D-55099 Mainz, Germany. E-mail: wolfrum@mail.uni-mainz.de

Received 4 January 1999; Accepted 13 March 2000

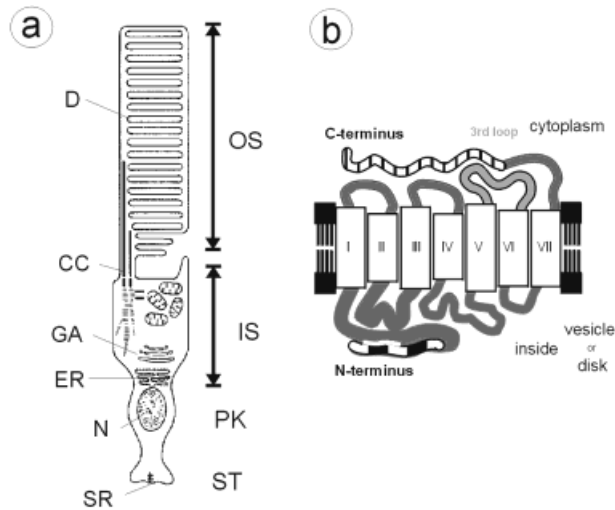


Fig. 1. Schematic representations of vertebrate rod photoreceptor cell (a) and rhodopsin (b). a: Vertebrate photoreceptor cells are divided into distinct anatomic compartments: The photosensitive outer segment (OS), which contains stacks of hundreds of membrane disks (D); the inner segment (IS), which contains the biosynthetic machinery, including the endoplasmic reticulum (ER), the Golgi apparatus (GA), and numerous of mitochondria; the perikaryon (PK), which contains the nucleus (N); and the synaptic terminal (ST) with the characteristic synaptic ribbons (SR). The only cytoplasmic linkage is between the OS and the IS the nonmotile connecting cilium (CC). b: The visual pigment rhodopsin is a G-protein-coupled 7-transmembrane receptor with its C-terminus facing the cytoplasm and its N-terminus directed into the lumen of transport vesicles or the outer segment disks. Monoclonal antibody (MAb) to bovine rhodopsin were used that recognize residues at the N-terminus and the C-terminus. As an unrelated peptide, a peptide of the sequence of the third cytoplasmic loop (gray) was used in preincubation assays.

that rhodopsin is transported in post-Golgi membrane vesicles to the base of the connecting cilium through the inner segment. Analysis of rhodopsin-bearing vesicles after subcellular fractionation of photoreceptor membranes showed that small G-proteins are apparently involved in the sorting of Golgi vesicles during their journey through the inner segment [for review, see Deretic and Papermaster, 1995]. Recent studies indicate that the C-terminal domain of rhodopsin is involved in the regulation of post-Golgi sorting [Deretic et al., 1998; Chuang and Sung, 1998] and, furthermore, that the directional trafficking is driven along the cellular microtubule network by cytoplasmic dynein interacting directly with the C-terminal domain of rhodopsin [Tai et al., 1999]. Although there is also considerable evidence that these rhodopsin-laden post-Golgi vesicles fuse with the plasma membrane of the apical inner segment at the periciliary region [Papermaster et al., 1985, 1986], the final step of rhodopsin delivery to the base of the outer segment remains unknown; the mechanism has remained an enigma for decades [Besharse and Horst, 1990].

Four different hypotheses have been under discussion: In Young's early studies, it was suggested that rhodopsin is transported through the cytoplasm of the lumen of the connecting cilium [Young, 1967, 1968; Young and Droz, 1969]. Subsequently, it was generally assumed that rhodopsin remains after its synthesis in the rough endoplasmic reticulum (rER) and during its trafficking through the inner segment in membrane compartments [Papermaster et al., 1985; see review Besharse, 1986]. Richardson [1969] assumed that rhodopsin is transferred via a cytosolic bridge between inner and outer segments occasionally observed by electron microscopy, but this linkage turned out to represent fixation artifacts [Besharse, 1986]. Most investigators have favored the ciliary membrane model for rhodopsin transport, which describes rhodopsin transport in the membrane of the connecting cilium of photoreceptors [Matsusaka, 1974; Röhlich, 1975; Besharse and Pfenninger, 1980; Nir and Papermaster, 1983; Peters et al., 1983; Papermaster et al., 1985; Besharse et al., 1985]. Although many research efforts have been directed toward a ciliary pathway for opsin delivery, as is commonly cited, clear direct evidence supporting the ciliary transport model was lacking [see review Besharse and Horst, 1990]. By contrast, the fourth hypothesis of an extracellular vesicular transport of rhodopsin has been supported by some experimental studies on amphibian photoreceptor cells [Besharse and Wetzel, 1995].

The present report provides striking evidence that rhodopsin is transported in the membrane of the connecting cilium from the inner segment to the outer segment of photoreceptor cells. Applying improved, highly sensitive immunoelectron microscopic labeling, in the membrane of the photoreceptor cilium, rhodopsin molecules are densely labeled by monoclonal antibodies against bovine rod opsin. Our studies show that during the ciliary passage of rhodopsin to the outer segment, rhodopsin colocalizes with myosin VIIa, the product of human Usher syndrome 1B gene. Furthermore, we have identified actin for the first time in the connecting cilium of photoreceptors. Membrane-associated dimers of the unconventional myosin VIIa act most probably as molecular motors for the ciliary membrane trafficking along axonemal actin filaments. Our present results also support the hypothesis that the symptoms of Usher syndrome are caused by defects in the function of sensory cilia [Barrong et al., 1992; Liu et al., 1997].

MATERIALS AND METHODS

Animals and Tissue Preparation

All experiments described in this report conform to the statement by the Association for Research in Vision

and Ophthalmology as to care and use of animals in research. Adult Sprague-Dawley albino rats and C57BL/6 mice were maintained on a 12/12 light/dark cycle with lights on at 6 a.m., and food and water ad libitum. After sacrifice of the animals in CO₂, retinas were removed through a slit in the cornea before fixation and embedding for electron microscopy or biochemical analysis. Bovine eyes were obtained from the local slaughterhouse and were kept on ice in the dark until further processing. The human retina processed in the present study was isolated from an eye of a 64-year-old female donor. The tenets of the Declaration of Helsinki were followed.

Antibodies

Monoclonal antibodies (MAbs) against bovine rod opsin were B6-30a1, K16-155, and R2-15, previously described by Adamus et al. [1988, 1991]. Epitope mapping has shown that B6-30a1 (N1) and R2-15 (N2) react with an N-terminal peptide, while K16-155 reacts with a C-terminal peptide (Fig. 1b). In immunological experiments, the anti-opsin monoclonals were applied separately or were used in a cocktail of all three clones (1:1:1), respectively.

Myosin VIIa antibodies were generated and purified as described by Liu et al. [1997]. In the present paper, we used antibodies made against a recombinant protein, corresponding to amino acids 941–1071 of mouse myosin VIIa. The antibody depicted in all the figures of the present paper is the one referred to as pAb 2.2 by Liu et al. [1997].

A mouse monoclonal antibody (MAb) against chicken gizzard actin (clone C4) has been previously characterized and used successfully in immunoelectron microscopy [Lessard, 1988; Wolfrum, 1991, 1997]. Mouse monoclonal antibodies against α -tubulin (clone DM 1A) and acetylated α -tubulin (clone 6-11B-1) were purchased from Sigma Chemical Co. (Deisenhofer, Germany).

Peptide Preincubation of Anti-Opsins

Although the MAb against bovine rod opsin used in the present study have been previously characterized by Adamus et al. [1988, 1989], additional tests for their specificity in rodent tissue were run. For control experiments, anti-opsin MAb were preincubated with specific peptides of the C-terminus (D-69 bovine rhodopsin (Brh) amino acids (aa) 324–348: GKNPLGDDEASTTVSK-TETSQVAPA) or the N-terminus (A-16 Brh aa 3–14: GTEGPNFYVPFS), respectively, as well as an unrelated peptide of the third cytoplasmic loop (D-70 Brh aa 231–252: KEAAAQQQESATTQKAEKEVTR) of bovine rod opsin diluted in PBS (1.5 mg/ml) for 1 h at room tem-

perature before immunological detection in Western blots or immunoelectron microscopy.

Western Blot Analysis

For Western blots, isolated retinas were homogenized and placed in sodium dodecyl sulfate-polyacrylamide gel electrophoresis (SDS-PAGE) sample buffer (62.5 mM Tris buffer, 10% glycerol, 2% SDS, 5% mercaptoethanol, 1 mM EDTA, 0.025 % bromophenol blue, pH 6.8). Proteins were separated by SDS-PAGE, transferred electrophoretically to Immobilon-P, blocked, and probed with primary and secondary antibodies [Wolfrum, 1995]. The latter was conjugated to alkaline phosphatase, so that labeling was detected by the formation of the insoluble product of 5-bromo-4-chloroindoyl phosphate hydrolysis.

Axoneme Preparation

Photoreceptor axonemes were purified from isolated bovine retinas, using sucrose density gradients in combination with cytoskeleton extraction according to Horst et al. [1987; Fleischman et al., 1980; Pagh-Roehl and Burnside, 1995]. The bovine retinas were isolated and suspended in 50% sucrose in HERT buffer (4 mM NaHCO₃, 0.18 mM sucrose, 2.1 mM HEPES, 0.1 mM ascorbic acid, 0.5 mM taurine, 1× Earle's balanced salt solution (EBSS) (Sigma), pH 7.5). After vigorous shaking for 1 min to shear off outer segments containing the connecting cilium, the photoreceptor fragments were isolated from the remainder of the retina by centrifugation on a 50% sucrose gradient in HERT buffer and purified in a second step, using a continuous 25–50% sucrose gradient in HERT buffer. Photoreceptor fragments were enriched by centrifugation on 50% sucrose in HERT buffer and sedimented by decreasing the sucrose concentration [cf. Fleischman et al., 1980; Horst et al., 1987; Pagh-Roehl and Burnside, 1995]. For cytoskeleton extractions, pellets were resuspended in a cytoskeleton extraction buffer (100 mM HEPES, 100 mM MgSO₄, 10 mM EGTA, 100 mM KCl, 1% dimethylsulfoxide (DMSO), 100 mM DTT, 0.5 mM GTP, 50 μ g phalloidin, 1 mM taxol, 1% Triton X-100, 24 μ M leupeptin, 0.2 mM PMSF, pH 7.4) and incubated for 1 h on ice. The axonemes were then isolated by centrifugation on a discontinuous sucrose gradient (40%, 50%, and 60% sucrose) in CMOD-buffer containing 100 mM HEPES, 10 mM MgSO₄, and 100 mM KCl (pH 7.4). Fractions of the gradient containing axonemes were analyzed by optic microscope, collected and placed in SDS-PAGE sample buffer. After transblotting, as above, immunoreactivity to the antibodies used was determined.

Immunoelectron Microscopy

Isolated retinas were fixed in 0.1% glutaraldehyde and 4% paraformaldehyde in 0.1 M phosphate buffer (pH

7.4) for 3 h at room temperature. Fixed tissue was dehydrated to 98% ethanol, embedded in LR White hard (Science Services, Munich, Germany), and polymerized at 4°C under ultraviolet (UV) light for 48–60 h.

Ultrathin sections (60–70 nm) were cut on a Leica Ultracut S and were collected on Formvar-coated nickel grids. Sections were first etched with saturated sodium periodate (Sigma) at room temperature for 3–5 min. The grids were preincubated with 0.1% Tween 20 in phosphate-buffered saline (PBS), then blocked with 50 mM NH₄Cl in PBS and in blocking solution (0.5% fish gelatin (Sigma) plus 0.1% ovalbumin (Sigma) in PBS). Sections were incubated with primary antibodies diluted in blocking solution at 4°C for 60 h, washed once in PBS and twice in a mixture of 0.1% ovalbumin, 0.5% cold-water fish gelatin, 0.01% Tween 20, 0.5 M NaCl in 10 mM phosphate buffer, pH 7.3 (IgG-gold buffer). The sections were incubated for 2 h with goat anti-mouse or anti-rabbit Fab conjugated to nanogold™ (Nanoprobes, Stony Brook, NY), diluted in IgG-gold buffer. Washed sections were postfixed in 2% glutaraldehyde for 10 min and air-dried. The nanogold™ labeling was silver-enhanced for 25 min at room temperature as described by Danscher [1981]. The grids were then washed in distilled water and stained with 2% ethanolic uranyl acetate for 10 min before examination in a Zeiss EM 912Ω, Zeiss EM 900, or LEO EM 906 electron microscope. For contrast enhancement, scattered electrons were analyzed using the Ω-filter system of the Zeiss EM 912Ω electron microscope in the zero-loose mode.

For immunoelectron microscopic double-labeling, ultrathin LR White sections through mouse retinae were incubated first with a cocktail of primary antibodies (mouse anti-opsins MAb and anti-myosin VIIa antiserum from rabbit) in blocking buffer at least for 60 h. To visualize antibody reaction sites, secondary antibodies conjugated to gold particles of different sizes (10 nm colloidal gold-coupled goat anti-rabbit IgG and goat anti-mouse Fab'-1.4 nm nanogold™ and vice versa (Nanoprobes or Aurion, Wageningen, The Netherlands) were applied mixed together in IgG-gold buffer. The time for silver enhancement of double-stained (1.4-nm and 10-nm gold particles) sections was reduced to 20 min.

Quantification of Immunolabeling

Immunoelectron microscopic labeling of different membrane regions and ciliary domains of rat photoreceptor cells were quantified by counting silver-enhanced gold particles on electron microscopic micrographs of ultrathin sections. Anti-opsin labeling of different membrane regions was determined from longitudinal sections through 30 photoreceptor cells of three rats. Data on ciliary domains were obtained from cross sections through 12 connecting cilia for the anti-myosin VIIa and

the anti-actin labeling, or through 17 connecting cilia for anti-opsin labeling, respectively from two rats.

RESULTS

Epitope mapping has shown that the MAbs used in the present study react with the specific domains of bovine rod opsin indicated in Figure 1b [Adamus et al., 1988, 1991]. The antibody clone K16-155 reacted with a peptide of the C-terminus, while the antibodies of the clones R2-15 and B6-30A1 bind to the N-terminal end of bovine opsin. To demonstrate their specificity in tissue of other mammals and on retinal sections, we have performed additional tests including preincubation of the antibodies with specific bovine opsin peptides.

Anti-Opsin Western Blot Analysis of Retinal Lysates

In Western blot analyses of retinal proteins of all mammalian species investigated (human, mouse, rat, bovine), a cocktail of all 3 MAbs to bovine rod opsin mixed together, as well as the three separate MAbs recognized two peptide bands, one at about 35 kDa, the estimated molecular weight of an opsin monomer and the higher-molecular-weight dimeric opsin commonly found after SDS-PAGE (Fig. 2). The labeling of opsin was inhibited when the C-terminal antibody (K16-155) was preincubated with the C-terminal peptide and when the N-terminal antibodies (R2-15; B6-30A1) were preadsorbed with the N-terminal peptide. By contrast, incubation of the C-terminal antibody was not inhibited with either the N-terminal peptide or a peptide of the third cytoplasmic loop of bovine opsin (loop-peptide). In addition, preadsorption of the N-terminal antibodies with neither C-terminal peptide nor the loop-peptide interfered with opsin recognition in retina lysates by the antibody (Fig. 2).

Anti-Opsin Immunolabeling of Photoreceptor Cells

In ultrathin sections of human and rodent retinae embedded in LR White, silver-enhanced immunogold labeling with MAb to bovine rod opsin was restricted to rod photoreceptor cells. By contrast, in cone photoreceptor cells, which express cone opsins different to rod opsin, the labeling was not above background staining (Fig. 3). In rod photoreceptor cells, most prominent labeling of opsin was observed as expected at disk membranes of outer segments (Figs. 3b,c, 4). Immunogold labeling of opsin was inhibited when the MAbs to opsin were preincubated with specific peptides (Fig. 4b). By contrast, preincubation with peptides unrelated to bovine opsin, as well as peptides of different opsin domains, did not inhibit immunogold staining of opsin (Figs. 3c, 4a,c). In rod photoreceptor cells, additional anti-rod-opsin la-

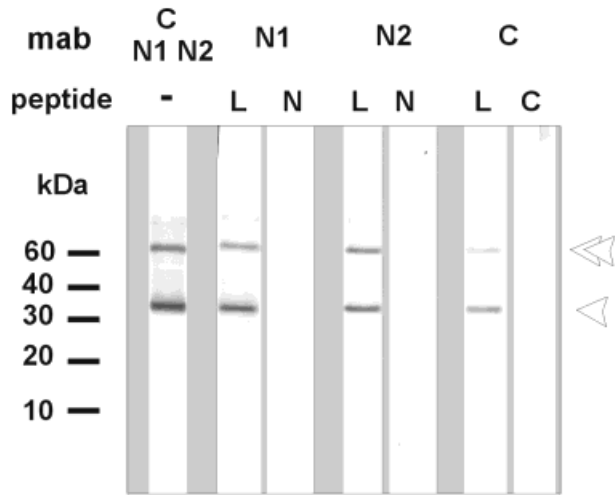


Fig. 2. Western blot analysis of monoclonal antibodies (MAbs) against bovine rod opsin in rat retina protein preparations. **Lane 1**, determination that the cocktail of 3 MAb (N1, N2, and C) recognizes opsin bands (arrowheads) in a rat retina protein sample; **lane 2**, labeled with N1 MAb B6-30a1 preincubation with the third loop peptide (L); **lane 3**, labeled with N1 MAb B6-30a1 after preincubation with the N-terminal peptide (N); **lane 4**, labeled with N2 MAb R2-15 preincubation with the third loop peptide (L); **lane 5**, labeled with N2 MAb R2-15 after preincubation with the N-terminal peptide (N); **lane 6**, labeled with C MAb K16-155 preincubation with the third loop peptide (L); **lane 7**, labeled with C MAb K16-155 after preincubation with the C-terminal peptide (C). Preadsorption of MAbs against opsin with the specific competitive peptide completely inhibits immunorecognition of opsin. Arrowhead indicates opsin monomers; double-arrowhead indicates artificially formed opsin dimers.)

being was present in the biosynthetic active membranes of the ER and the Golgi apparatus as well as at the apical domains of the cytoplasmic membrane of inner segments. Moreover, applying our highly sensitive detection method of silver-enhanced nanogold™ labeling, in contrast to previous investigations (see introduction), dense labeling of rod opsin was also observed in the membrane of the connecting cilium in wild type mammals and human (Fig. 4a,c). While the MAb against the N-terminal domain (clones R2-15 and B6-30A1) show about the same dense labeling, clone K16-155 directed against the C-terminal of bovine opsin stains the ciliary membrane much weaker (data not shown), indicating that C-terminal epitopes of some opsin molecules are probably masked by associated molecules. Therefore, for quantification purposes, longitudinal sections through rat photoreceptor cells were labeled with the anti-opsin MAb cocktail composed of MAbs against C- and N-terminal domains. For this quantification of immunogold labeling of opsin, the number of silver-enhanced gold particles per membrane μm were determined at different domains of the photoreceptor membrane (Fig. 5a). To confirm the localization of rhodopsin in the membrane of the con-

necting cilium of photoreceptor cells, we have also determined the number of silver-enhanced gold particles per ciliary cross section of different subciliary domains of the rod connecting cilium. The quantitative results are shown in Figure 5b. Our investigations showed that opsin was most abundant in the outer segment disk membrane. However, in comparison, the membrane of the connecting cilium displayed significantly more, about 2.5-fold more, rhodopsin than the membrane of the apical inner segment.

Western blot analysis of proteins of an axonemal preparation from isolated bovine photoreceptor cells demonstrates that the cocktail of the three MAb to bovine opsin epitopes also recognizes two opsin bands (Fig. 6, lane 2). Since *trans*-membrane proteins including opsin are commonly extracted by detergents, the remaining of opsin in the detergent-treated cytoskeletal fraction is unusual and may indicate an association with cytoskeletal proteins of the cilium.

Myosin VIIa Is a Membrane-Associated Motor Protein in the Photoreceptor Cilium

Given a ciliary pathway of the intersegmental transport of rhodopsin in photoreceptor cells, the question of which molecular motors are involved in this ciliary membrane transport arises. In vertebrate photoreceptor cells, several members of the superfamily of kinesins have been immunocytochemically localized at the connecting cilium [Beech et al., 1996; Muresan et al., 1997]. However, a convincing direct association of a motor protein with the ciliary membrane in mammalian photoreceptors has only been shown for the unconventional myosin VIIa [Liu et al., 1997; present study] (Figs. 7, 8). In the present study, quantification of silver-enhanced immunogold labeling of myosin VIIa in ultrathin transversal sections through rat photoreceptor cilia provided additional evidence for myosin VIIa linkage with the ciliary membrane and the spatial vicinity to rhodopsin pathing through the ciliary membrane (Fig. 5c). Quantitative evaluation of silver-enhanced gold particles in different domains of the connecting cilium revealed that myosin VIIa localization is almost exclusively restricted to the ciliary membrane domain while any labeling of myosin VIIa in the ciliary lumen was absent.

Verification of Ciliary Myosin VIIa/Rhodopsin Co-localization by Immunoelectron Microscopic Double-Labeling

To confirm that myosin VIIa and rhodopsin were spatially associated at the membrane domain of the photoreceptor connecting cilium, immunoelectron microscopic double-labeling with anti-myosin VIIa serum and anti-opsin MAbs were performed. For the discrimination between reaction sites of both types of immunochemi-

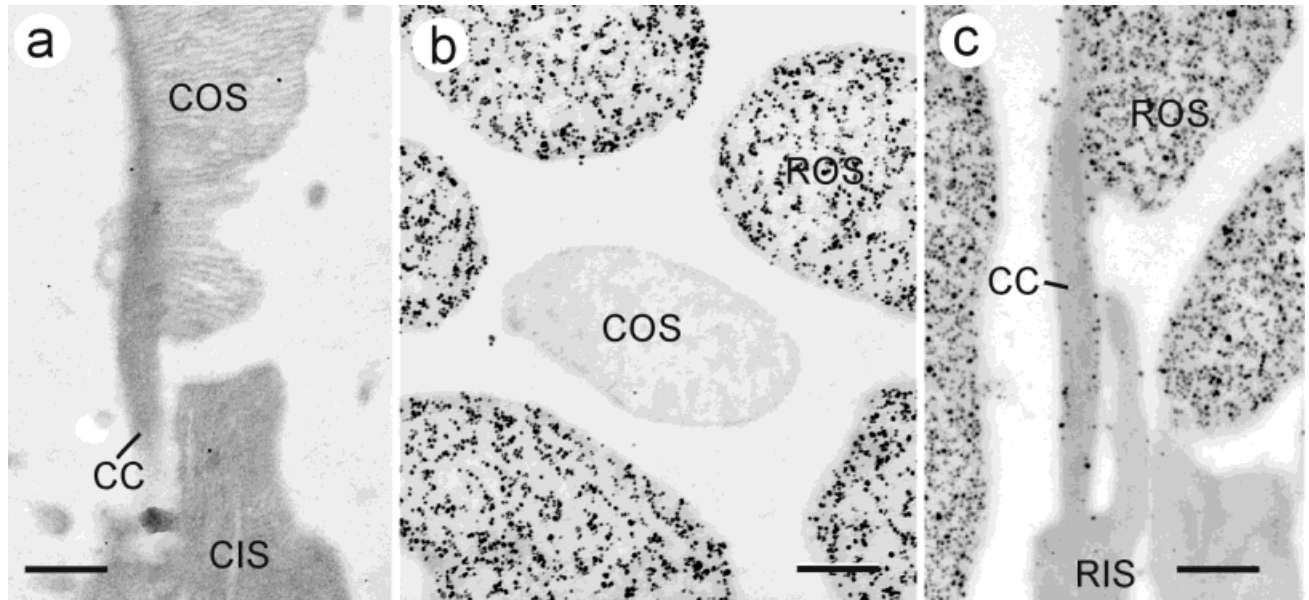


Fig. 3. Immunoelectron microscopic localization of rod rhodopsin in rat photoreceptor cells. **a:** Longitudinal section of part of a rat cone photoreceptor cell. **b:** Transverse section at the plane of photoreceptor outer segments. **c:** Longitudinal section of part of a rat rod photoreceptor cell. In ultrathin sections, the cocktail of the monoclonal antibody (MAb) B6-30a1, R2-15, and K16-155 against rod bovine opsin specifically recognizes rhodopsin in rat rod cells. Silver-enhanced

immunogold labeling is restricted to rod photoreceptors. By contrast, in cones, labeling is not above background staining. In rods, rhodopsin is most intensely present in disk membranes of rod outer segments (ROS), but is also localized in the membrane of the connecting cilium (CC). Cone inner segment (CIS); rod inner segments (RIS); cone outer segment (COS). Scale bars = 200 nm (a); 200 nm (b); 170 nm (c).

icals, secondary antibodies conjugated to gold particles of different sizes, nanogold™ probes (1.4-nm) and 10-nm colloidal gold, were used. Electron microscopic analysis of double-labeled ultrathin sections through mouse photoreceptor cells convincingly demonstrated co-localization of myosin VIIa and rhodopsin at the membrane of the connecting cilium (Fig. 8).

Actin Localization at the Ciliary Membrane

We reasoned that, as in all known myosins, the myosin VIIa motile function should also be based on the interaction with actin filaments. Previous studies by others have been demonstrated actin filaments at the base of the photoreceptor outer segment [Chaitin et al., 1984; Chaitin and Bok, 1986; Arikawa and Williams, 1989; Chaitin and Burnside, 1989; Obata and Usukura, 1992; Usukura and Obata, 1995], where they are supposed to be involved in disk formation interacting with conventional myosin II [Chaitin and Coelho, 1992; Williams et al., 1992]. In Western blot analysis of axonemal preparations from bovine photoreceptor cells a 42-kDa band was recognized by the well-characterized MAb to actin (clone C4) (Fig. 6, lane 4). Moreover, present immunoelectron microscopy provided first evidence for a membrane-linked actin cytoskeleton in photoreceptor cilia. In highly sensitive silver-enhanced immunogold labeling of

rat photoreceptor sections by anti-actin MAbs, the actin localization was not restricted to the apical portion of the connecting cilium at the base of the outer segment but was also present at the cytoplasmic surface of the entire ciliary membrane (Fig. 9). For quantification, the number of silver-enhanced gold particles of anti-actin labeling were determined per ciliary cross section. The histogram presented in Figure 5d shows that in the connecting cilium, most anti-actin label was localized at the ciliary membrane.

DISCUSSION

Rhodopsin is Translocated in the Membrane of the Connecting Cilium to the Photoreceptor Outer Segment

Transport of rhodopsin from the inner segment to the outer segment of vertebrate photoreceptor cells has been one of the major remaining mysteries of photoreceptor cell biology and has been a source of controversial discussion for decades [Besharse and Horst, 1990]. In the absence of direct immunocytochemical evidence for a ciliary pathway, the prevailing dogma has given preference to an extracellular vesicular transport [Besharse, 1986; Besharse and Wetzel, 1995]. Our results reveal

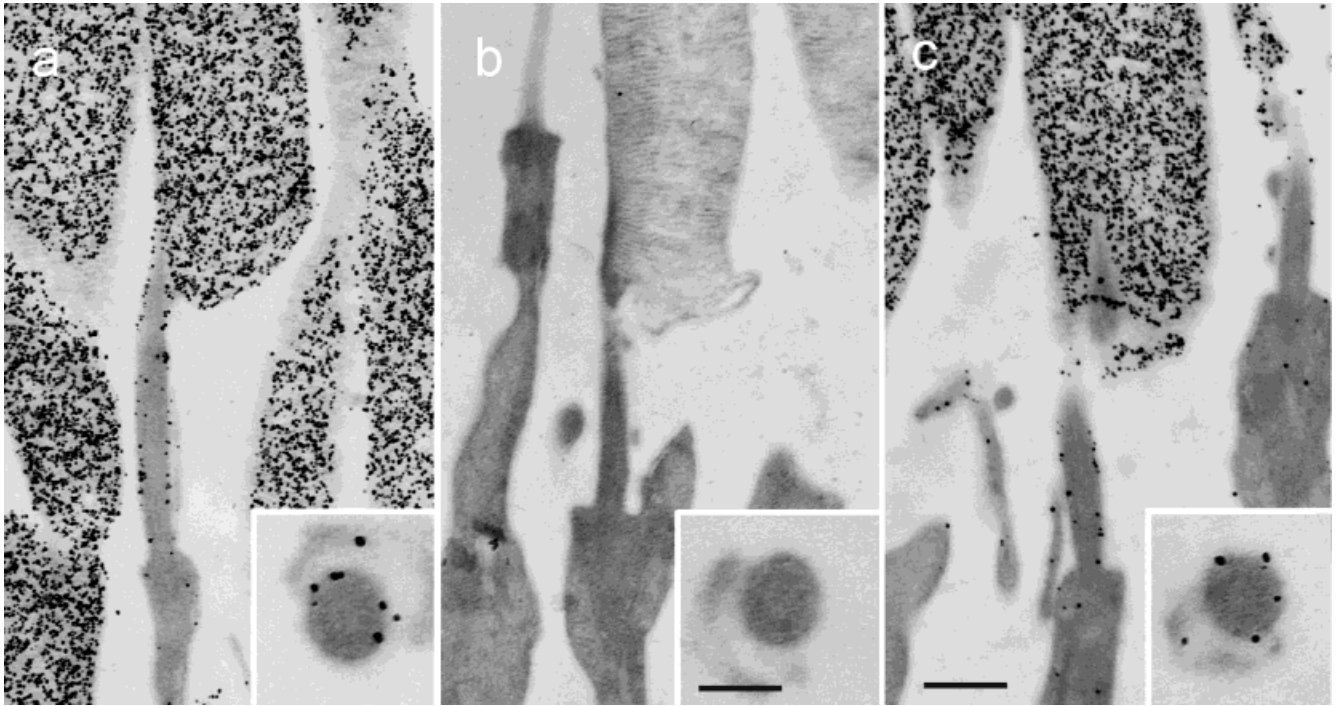


Fig. 4. Immunoelectron microscopic analysis of the monoclonal antibody (MAb) N2 (clone R2-15) against rod bovine opsin on ultrathin sections of rat rod photoreceptors. Longitudinal section of part of a rat rod photoreceptor cell and transverse sections through the connecting cilium (insets) silver-enhanced immunogold by MAb N2 (clone R2-15) (a) preincubated with the C-terminal peptide of bovine opsin, (b) preincubated with the N-terminal peptide of bovine opsin, and (c) preincubated with the third cytoplasmic loop peptide of bovine opsin.

Preincubation of MAb N2 with either the C-terminal peptide (a) or the third cytoplasmic loop peptide and (c) has no effect on opsin recognition in rat photoreceptors: MAb N2 (clone R2-15) most intensely label the disk membranes in the rod outer segment but also stains the membrane of photoreceptor connecting cilia in longitudinal and transverse ciliary sections. Preincubation with the specific competitive N-terminal peptide completely inhibits immunoreactivity of MAb N2 (clone R2-15) (b). Scale bars = 250 nm; 125 nm (insets).

that rhodopsin is also present as an integral membrane protein in the photoreceptor connecting cilium. Weak rhodopsin labeling in the photoreceptor cilium has previously been reported by several authors [e.g., Papermaster and Schneider, 1982; Nir et al., 1984, 1987, 1989; Nir and Papermaster, 1983, 1986, 1989; Hicks and Barnstable, 1986; Besharse et al., 1985]. These reports of weak opsin immunoreactivity in the ciliary membrane have been a major obstacle to accepting a ciliary transport of rhodopsin [Besharse, 1986; Besharse and Horst, 1990].

In contrast to previous studies, the sensitivity of immunoelectron microscopy has been increased by a combination of several technical improvements, in the present investigation. To minimize steric interference of colloidal gold particles coupled to secondary antibodies, ultra small gold probes (nanogold) were used for immunolabeling, which were visualized for biological electron microscopy by silver enhancement. In addition, etching of the LR White ultrathin sections before postembedding immunogold labeling should increase the number of antigenic epitopes presented at the surface of the ultrathin

section. Furthermore, to avoid the physiological epitope masking of rhodopsin in the ciliary membrane by associated molecules which were previously discussed [Besharse et al., 1985; Bok, 1985], we used a cocktail of MAbs against opsin or MAbs against the N-terminal of opsin which should be exposed at the extracellular face of the ciliary membrane. In addition, using Western blot analysis as well as immunoelectron microscopy, the present experiments of peptide preincubation of the bovine rod opsin MAbs demonstrate high epitope specificity of the MAbs employed. Previous estimations found the number of opsin molecules in the connecting cilium of wild-type photoreceptors to be too small for intense immunoelectron microscopic labeling [Liu et al., 1999]. However, our methodology modifications have permitted visualization of rhodopsin by immunoelectron microscopy, not only in the membranes of inner and outer segments, but also, for the first time, densely localized in the membrane of photoreceptor connecting cilia of wild-type mammals, including human. The cocktail of MAb of bovine rod opsin and the MAb against the N-terminus of bovine rod opsin also react significantly with rhodop-

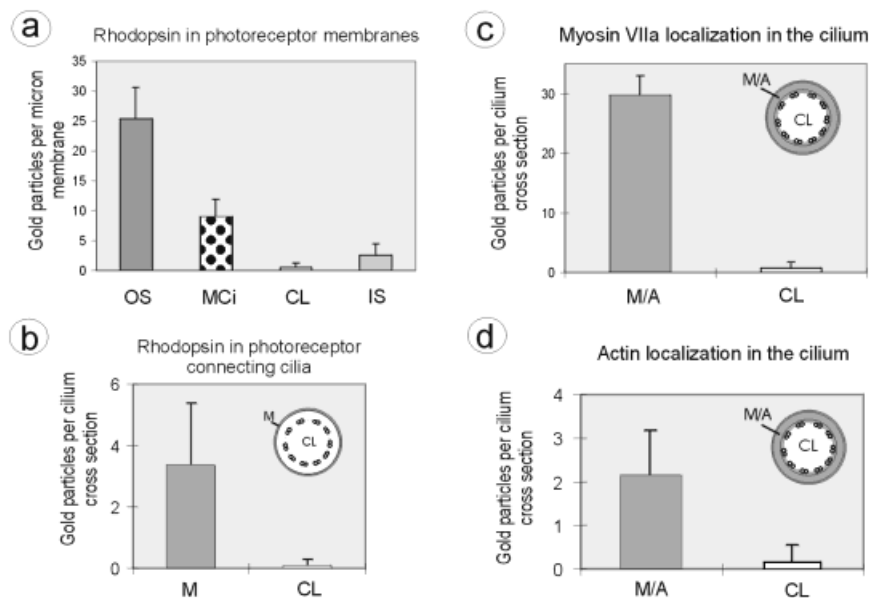


Fig. 5. Histograms of quantitative analysis of immunoelectron microscopic localization. **a**: Silver-enhanced gold particle counts of anti-opsin immunolabeling at membrane domains and the cilium of rat rod photoreceptor cells. Histogram indicates mean number of gold particles per μm membrane. **b**: Silver-enhanced gold particle counts of anti-opsin immunolabeling at domains of the connecting cilium of rat rod photoreceptor cells. Histogram indicates mean number of gold particles per cilium transverse section. **c**: Silver-enhanced gold particle counts of anti-myosin VIIa immunolabeling at domains of the con-

necting cilium of rat rod photoreceptor cells. Histogram indicates mean number of gold particles per cilium transverse section. **d**: Silver-enhanced gold particle counts of anti-actin immunolabeling at domains of the connecting cilium of rat rod photoreceptor cells. Histogram indicates mean number of gold particles per cilium transverse section. CL, ciliary lumen; M/A, domain of ciliary membrane, including ciliary submembrane domains; OS, outer segment disk membrane; Mci, ciliary membrane; IS, inner segment membrane; M, ciliary membrane. Error bars = standard error of the mean.

sin in the connecting cilium, showing that the ciliary rhodopsin is not in a nonimmunoreactive conformation, as suggested by Hicks and Barnstable [1986, 1987] to explain weak anti-opsin staining. The present Western blot analysis of axonemal protein preparation of bovine photoreceptor cells may further support the ciliary transport of rhodopsin.

We conclude, on the basis of immunoelectron microscopy, that the numerous rhodopsin molecules we have detected as integral membrane proteins in the connecting cilium are on their passage through the cilium from the inner segment to the base of the outer segment of photoreceptor cells. We have gathered significant evidence for the ciliary membrane pathway of rhodopsin transport between the inner and outer segment, which has been predicted from early biological electron microscopic examination of retinal cells. Our results are consistent with observation by confocal microscopy showing strong anti-opsin immunofluorescence at the connecting cilium [Matsumoto and Hale, 1993]. Further confirmation of our data comes from results obtained by freeze-fracture experiments indicating the presence of particles in the ciliary membrane of photoreceptors that are similar in shape and size to rhodopsin particles localized in the disk membrane of outer segments [Matsusaka, 1974;

Röhlich, 1975; Besharse and Pfenninger, 1980; Roof and Heuser, 1982; Besharse et al., 1985; Miyaguchi and Hashimoto, 1992]. In addition, investigations on shaker1 mouse mutants showed that rhodopsin is present in the ciliary membrane in photoreceptors gathered under artificial pathological conditions [Liu et al., 1999] (C. Bode and U. Wolfrum, unpublished observations).

Molecular Motors Supporting the Vectorial Transport of Rhodopsin Through the Connecting Cilium

Given that rhodopsin is translocated from the inner segment to the outer segment via the connecting cilium incorporated in the ciliary membrane, an efficient mechanism for the unidirectional delivery of membrane components through the ciliary membrane must exist. Quantitative analysis of the components involved in disk assembly reveals that in the development as well as in the renewal of outer segments, throughout lifetime of mammalian photoreceptor cells, 2000 rhodopsin molecules and $0.1 \mu\text{m}^2$ of membrane per minute must pass through the short and slender cilium (in mammals, the cilium measures about $1 \mu\text{m}$ in longitudinal extension and $<0.2 \mu\text{m}$ in diameter) [Besharse, 1986]. To realize such highly directed rhodopsin transport, cellular motor proteins

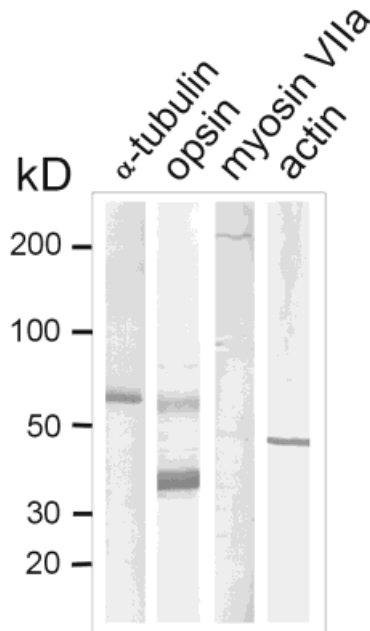


Fig. 6. Immunoblot analysis of photoreceptor axonemes. Western blots were probed with antibodies against α -tubulin (**lane 1**), opsin MAb cocktail (**lane 2**), myosin VIIa (**lane 3**), and actin (**lane 4**) after SDS-PAGE protein-separation of the cytoskeleton fraction of purified photoreceptor axonemes isolated from bovine retinae. All four antibodies recognize polypeptides at expected molecular weight.

likely contribute in the ciliary trafficking of rhodopsin. Recently we have shown that a dynein light chain binds directly to the C-terminus of rhodopsin and proposed that in the inner segment, cytoplasmic dynein mediates the microtubule-based minus-end directed vectorial translocation of rhodopsin bearing vesicles from the post-Golgi network to the basal body region at base of the connecting cilium [Tai et al., 1999]. However, the molecular motor system to which rhodopsin is handed over from the cytoplasmic dynein for its passage through the connecting cilium has not yet been identified. Since microtubules are the characteristic cytoskeletal elements in ciliary axonemes, plus-end directed microtubule-based transport molecules are attractive candidates for the ciliary transport. Indeed, in cilia of vertebrate photoreceptors, members of the kinesin superfamily proteins (KIFs) have been identified [Beech et al., 1996; Muresan et al., 1997; Whitehead et al., 1999]. Therefore, these microtubule-based plus-end-directed mechanochemical motors have been suggested to contribute to rhodopsin transport in the photoreceptor cilium. Recent studies on KIF3A conditional knock out mice show that KIF3A is indeed required for the normal renewal of outer segment membranes [Marszalek et al., 1998; Williams et al., 1999]. However, the ciliary transport of integral membrane protein rhodopsin does not seem to be affected in KIF3A-

deficient mice, indicating that rhodopsin transport and disk membrane formation at the outer segment are controlled by separate mechanisms [Marszalek et al., 1998; Williams et al., 1999].

Another candidate for motor protein contributing to ciliary transport is myosin VIIa that has been localized to the membrane of mammalian photoreceptor connecting cilia [present paper; and Liu et al., 1997, 1999; Wolfrum and Schmitt, 1999]. Myosin VIIa is an unconventional myosin with characteristic functional domains: the head, the neck, and the tail domain. Talin-like sequence motifs at the tail domain are responsible for membrane binding, whereas in the neck domain, a coiled-coil motif indicates dimer formation [Chen et al., 1996; Weil et al., 1996; Mburu et al., 1997]. The mechanochemical ATPase function of the head domain of myosin motors is based on filamentous actin [Hasson and Mooseker, 1997].

Actin is Spatially Co-localized With Myosin VIIa in the Connecting Cilium

Actin filaments have been identified at the distal cilium in the base of the outer segment by several authors [e.g., Chaitin et al., 1984; Chaitin and Bok, 1986; Arikawa and Williams, 1989; Chaitin and Burnside, 1989; Obata and Usukura, 1992; Usukura and Obata, 1995]. However, in the distal portion of the cilium, myosin VIIa is absent [Liu et al., 1997] and the actin filaments may interact with conventional myosin II [Chaitin and Coelho, 1992; Williams et al., 1992]. In contrast, in the proximal portion of the cilium, although weak immunogold labeling at the ciliary membrane is visible in previously published photographs [for example see Figure 8 in Arikawa and Williams, 1989], it has not been considered to be of functional significance. Our present highly sensitive immunolabeling by nanogoldTM probes clearly indicated actin localization at the membrane of the connecting cilium. Localization of actin in the photoreceptor cilium is supported by the present Western blot analysis of axonemal protein preparations of bovine photoreceptor cells. It is also consistent with the identification of an actin-like protein in the axoneme of the flagellum of the green algae *Chlamydomonas* [Piperno and Luck, 1979]. Current immunoelectron microscopic techniques using MAb against actin do not discriminate between monomeric G-actin and actin filaments, and the resolution of light microscopic analysis with fluorescent phalloidins is not high enough to identify filamentous actin in subdomains of the slender cilium; however, we suggest that the actin molecules detected at the ciliary membrane form single filaments, which are common cytoskeletal elements in the membrane skeleton of eukaryotic cells [Isenberg and Niggli, 1998]. In the connecting cilium of photoreceptor cells, ciliary actin most probably forms filaments that run un-

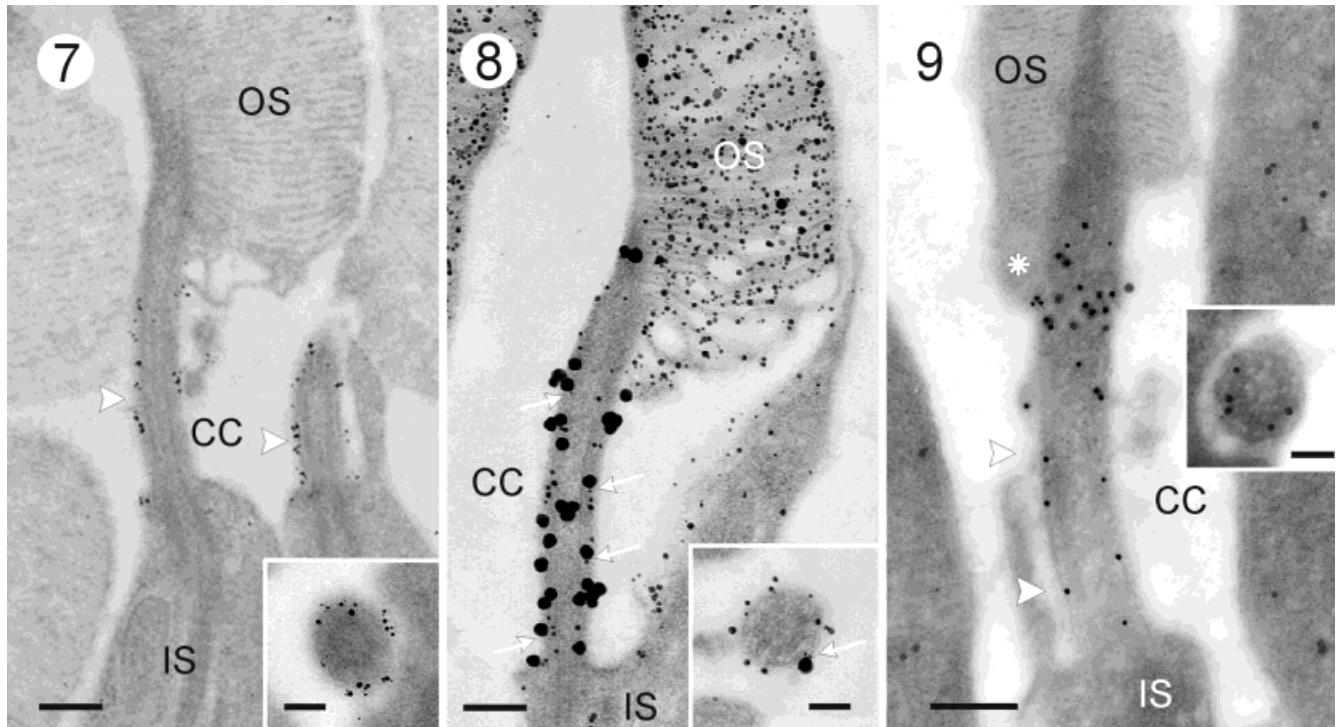


Fig. 7. Localization of myosin VIIa in the photoreceptor connecting cilium (CC). Silver-enhanced immunogold labeling of myosin VIIa in a longitudinal section of part of a mouse rod photoreceptor cell. **Inset:** transversal section through the photoreceptor connecting cilium. The proximal connecting cilium is labeled at the plasma membrane. IS, inner segment; OS, outer segment; Scale bars = 150 nm; 50 nm (inset).

Fig. 8. Co-localization of opsin and myosin VIIa in the photoreceptor connecting cilium (CC). Silver-enhanced immunogold double labeling of opsin (small particles) and myosin VIIa (large particles) in a longitudinal section of part of a mouse rod photoreceptor cell. **Inset:** Transversal section through a rod photoreceptor connecting cilium. Opsin and myosin VIIa are co-localized at the CC, indicated by white arrows. Scale bars = 100 nm; 50 nm (inset).

Fig. 9. Localization of actin in the photoreceptor connecting cilium (CC). Silver-enhanced immunogold labeling of actin in a longitudinal section of part of a rat rod photoreceptor cell. **Inset:** Silver-enhanced immunogold labeling of actin in a transverse section through the connecting cilium of a rat rod cell. Actin filaments are labeled at the base of the outer segment (OS) (asterisk) previously described by several investigators (see text). Applying present high sensitive immunolabeling by ultrasmall nanogoldTM probes in combination with silver-enhancement, actin is also recognized at the membrane of the CC (arrowheads). IS, inner segment. Scale bars = 150 nm; 50 nm (inset).

derneath the plasma membrane parallel to the axonemal microtubule doublets in a longitudinal orientation.

Actin-Based Motility of Myosin VIIa Contributes to Ciliary Transport of Rhodopsin

We conclude that, in addition to the characteristic axonemal microtubule cytoskeleton, in photoreceptor cilia, an actin-based cytoskeleton is present that permits myosin motor activity. Myosin VIIa may move with their actin-binding motor domain along axonemal actin filaments pulling membrane plaques attached to the myosin VIIa tail. This role of myosin VIIa in ciliary membrane trafficking in photoreceptor cells is also supported by studies on mechanosensitive hair cells in the cultured organs of Corti, which indicate an involvement of myosin VIIa in membrane translocalizations during hair cell differentiation [Richardson et al., 1997]. Present immu-

noelectron microscopic double-labeling experiments demonstrate that myosin VIIa and rhodopsin are spatially co-localized in the membrane domain of the connecting cilium, indicating functional coupling of myosin VIIa motor function and the transport of rhodopsin through the connecting cilium. In addition, in studies of developmental stages of rat photoreceptor cells, myosin VIIa labeling of the ciliary membrane interestingly occurs first at day 14 postnatal, just at the time when transport of rhodopsin to the outer segment begins (C. Bode and U. Wolfrum, unpublished observations). Further evidence for a direct role of myosin VIIa in ciliary rhodopsin transport comes from studies on shaker1 mice with different mutations in the myosin VIIa gene [Liu et al., 1999]. In homozygous mutants, an abnormal accumulation of rhodopsin has been recently described by Liu et al. [1999]. These findings are consistent with our unpub-

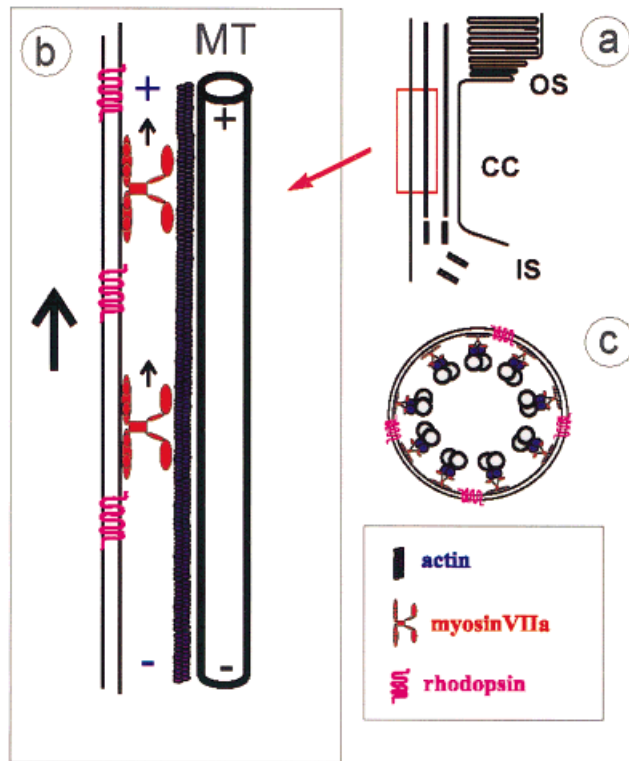


Fig. 10. Schematic representation of a rod photoreceptor cell illustrating the hypothesis of rhodopsin transport through the connecting cilium. **a:** Diagram of the ciliary joint between the inner segment (IS) and outer segment (OS). **b:** Enlargement of the membrane and associated cytoskeleton compositions. **c:** Scheme of a transverse section through the connecting cilium. Distribution of opsin, myosin VIIa, and actin is shown by immunoelectron microscopy. Rhodopsin-containing membrane plaques are transported in the plasma membrane of the connecting cilium to the base of the outer segment, where the membrane is incorporated into newly formed disks. This transport is probably driven by myosin VIIa moving along axonemal actin filaments (small arrows). Large arrows indicate the direction of the rhodopsin trafficking in the plasma membrane of the connecting cilium (CC). MT, axonemal microtubule; +, -, polarity of cytoskeletal elements.

lished results gathered in parallel experiments (C. Bode and U. Wolfrum, unpublished observations). Our present working hypothesis of the rhodopsin transport in the ciliary membrane of photoreceptor cells is illustrated in Figure 10. Although direct interaction between myosin VIIa and rhodopsin has not been demonstrated, both proteins may be components of a transport complex probably associated with additional proteins. However, it is also possible that myosin VIIa binds via the talin-like domains at its tail directly to the acid phospholipids of the ciliary membrane and transports membrane plaques, including membrane proteins without any physical contact to them.

If myosin VIIa translocates cargoes along the ciliary membrane with a velocity similar to that of other

dimeric unconventional myosins (e.g., myosin V), cargoes should be transported at about $0.5 \mu\text{m/s}$ [Wolenski et al., 1995]. Estimations by Liu et al. [1999] indicate that an average of about 150 rhodopsin molecules pass the cilium at each time, out of which, in the present study, at least one-fifth were decorated by the MAbs against the N-terminus of opsin. The high number of silver-enhanced immunogold particles counted for the present quantitative evaluation of immunoreactivity of the antibodies against myosin VIIa indicates that, if each myosin VIIa molecule is recognized by a single polyclonal antibody to myosin VIIa, at least one myosin VIIa dimer per opsin molecule is localized in the connecting cilium. However, even in myosin VIIa null mutants, rhodopsin still reaches the outer segment of the photoreceptor cell indicating that there is not a complete dependence on myosin VIIa and perhaps some redundancy amongst molecular motors transporting rhodopsin [Liu et al., 1999].

Blindness in Usher 1B Patients Probably Results From Defective Ciliary Transport of Rhodopsin

Previous reports indicate that patients with Usher syndrome have structural abnormalities in the cilia of the neuronal retina and other tissues [Arden and Fox, 1979; Hunter et al., 1986; Barrong et al., 1992]. Because all these structural changes might be caused by defects in ciliary function, it has been suggested that ciliary dysfunction might be the basis of the degenerative processes experienced by patients with Usher syndrome [Hunter et al., 1986]. Our results are consistent with this hypothesis: The *retinitis pigmentosa* in Usher 1B patients carrying mutated myosin VIIa genes might result from a defective ciliary transport of outer segment components by non-functional myosin VIIa. The failure of proper rhodopsin transport could also cause some other types of *retinitis pigmentosa* [Roof et al., 1994; Sung et al., 1994; Tai et al., 1999].

In conclusion, we have gathered striking evidence that, in mammalian photoreceptor cells, rhodopsin is transported in the membrane of the connecting cilium from the inner segment to the outer segment. Furthermore, we have identified a motile system based on actin and myosin VIIa at the membrane of the photoreceptor connecting cilium and suggest that this system contributes to rhodopsin translocation in the plasma membrane of the photoreceptor cilium. The dysfunction of ciliary transport in photoreceptor cells may underlie the *retinitis pigmentosa* found in Usher syndrome 1B patients. It will be interesting to determine whether in photoreceptor cilia, myosin VIIa forms a complex with rhodopsin and additional associated proteins, which other motor proteins also contribute to ciliary trafficking of rhodopsin, and how these processes are regulated.

ACKNOWLEDGMENTS

The present study is supported by the Deutsche Forschungs Gemeinschaft, grant Wo 548/3, Forschung Contra Blindheit-Initiative Usher Syndrome V, and the FAUN-Stiftung, Nürnberg, Germany (to U.W.). The authors are most grateful to Drs Paul A. Hargrave and Anatol Arendt (University of Florida, Gainesville, USA), for kindly supplying antibodies and peptides to bovine rod opsin. We thank Rainer Müller (University of Karlsruhe, Germany), for skillful technical assistance, and Christian Bode (University of Mainz, Germany), for his help with immunoelectron microscopic double labeling. We also thank Brenda K. Huntley (Mayo Foundation, Rochester, MN) for helpful comments on the manuscript and attentive linguistic corrections.

REFERENCES

- Adamus G, Arendt A, Zam ZS, McDowell JH, Hargrave PA. 1988. Use of peptides to select for anti-rhodopsin antibodies with desired amino acid sequence specificities. *Peptide Res* 1:42–47.
- Adamus G, Zam ZS, Arendt A, Palczewski K, McDowell JH, Hargrave PA. 1991. Anti-rhodopsin monoclonal antibodies of defined specificity: characterization and application. *Vision Res* 31:17–31.
- Arden GB, Fox B. 1979. Increased incidence of abnormal nasal cilia in patients with retinitis pigmentosa. *Nature* 279:534–536.
- Arikawa K, Williams DS. 1989. Organization of actin filaments and immunocolocalization of alpha-actinin in the connecting cilium of rat photoreceptors. *J Comp Neurol* 288:640–646.
- Barrong SD, Chaitin MH, Fliesler SJ, Possin DE, Jacobson SG, Milam AH. 1992. Ultrastructure of connecting cilia in different forms of retinitis pigmentosa. *Arch Ophthalmol* 110:706–710.
- Beech PL, Pagh-Roehl K, Noda Y, Hirokawa N, Burnside B, Rosenbaum JL. 1996. Localization of kinesin superfamily proteins to the connecting cilium of fish photoreceptors. *J Cell Sci* 109:889–897.
- Besharse JC. 1986. Photosensitive membrane turnover: differentiated membrane domains and cell-cell interaction. In: Adler R, Farber D, editors. *The retina: a model for cell biological studies*. San Diego, CA: Academic Press. p 297–352.
- Besharse JC, Pfenninger KH. 1980. Membrane assembly in retinal photoreceptors. I. Freeze-fracture analysis of cytoplasmic vesicles in relationship to disc assembly. *J Cell Biol* 87:451–463.
- Besharse JC, Horst CJ. 1990. The photoreceptor connecting cilium—a model for the transition zone. In: Bloodgood RA, editor. *Ciliary and flagellar membranes*. New York: Plenum. p 389–417.
- Besharse JC, Wetzel MG. 1995. Immunocytochemical localization of opsin in rod photoreceptors during periods of rapid disc assembly. *J Neurocytol* 24:371–388.
- Besharse JC, Forestner DM, Defoe DM. 1985. Membrane assembly in retinal photoreceptors. III. Distinct membrane domains of the connecting cilium of developing rods. *J Neurosci* 5:1035–1048.
- Bok D. 1985. Retinal photoreceptor-pigment epithelium interactions. *Invest Ophthalmol Visual Sci* 26:1659–1694.
- Chaitin MH, Bok D. 1986. Immunoferritin localization of actin in retinal photoreceptors. *Invest Ophthalmol Visual Sci* 27:1764–1767.
- Chaitin MH, Burnside B. 1989. Actin filament polarity at the site of rod outer segment disk morphogenesis. *Invest Ophthalmol Visual Sci* 30:2461–2469.
- Chaitin MH, Coelho N. 1992. Immunogold localization of myosin in the photoreceptor cilium. *Invest Ophthalmol Visual Sci* 33:3103–3108.
- Chaitin MH, Schneider BG, Hall MO, Papermaster DS. 1984. Actin in the photoreceptor connecting cilium: Immunocytochemical localization to the site of outer segment disk formation. *J Cell Biol* 99:239–247.
- Chen ZY, Hasson T, Kelley PM, Schwender BJ, Schwartz MF, Ramakrishnan M, Kimberling WJ, Mooseker MS, Corey DP. 1996. Molecular cloning and domain structure of human myosin VIIa. The gene product defective in usher syndrome 1B. *Genomics* 36:440–448.
- Corless JM, Cobbs WH, Costello MJ, Robertson JD. 1976. On the asymmetry of frog retinal rod outer segment disk membranes. *Exp Eye Res* 23:295–324.
- Danscher G. 1981. Localization of gold in biological tissue. A photochemical method for light and electron microscopy. *Histochemistry* 71:81–88.
- Deretic D, Papermaster DS. 1995. The role of small G-proteins in the transport of newly synthesized rhodopsin. *Prog Retin Eye Res* 14:249–265.
- Deretic D, Schmerl S, Hargrave PA, Arendt A, McDowell JH. 1998. Regulation of sorting and post-Golgi trafficking of rhodopsin by its C-terminal sequence QVS(A)PA. *Proc Natl Acad Sci USA* 95:10620–10625.
- Fleischman D, Denisevich M, Raveed D, Pannbacker RG. 1980. Association of guanylate cyclase with the axoneme of retinal rods. *Biochim Biophys Acta* 630:176–186.
- Gibson F, Walsh J, Mburu P, Varela A, Brown KA, Antonio M, Beisel KW, Steel KP, Brown SDM. 1995. A type VII myosin encoded by the mouse deafness gene shaker-1. *Nature* 374:62–64.
- Hall MO, Bok D, Bacharach ADE. 1969. Biosynthesis and assembly of the rod outer segment membrane system. Formation and fate of visual pigment in the frog retina. *J Mol Biol* 45:397–406.
- Hasson T, Mooseker MS. 1997. The growing family of myosin motors and their role in neurons and sensory cells. *Curr Opin Neurobiol* 7:615–623.
- Hicks D, Barnstable CJ. 1986. Lectin and antibody labelling of developing rat photoreceptor cells: an electron microscope immunocytochemical study. *J Neurocytol* 15:219–130.
- Hicks D, Barnstable CJ. 1987. Different rhodopsin monoclonal antibodies reveal different binding patterns on developing and adult rat retina. *J Histochem Cytochem* 35:1317–1328.
- Horst CJ, Forestner DM, Besharse JC. 1987. Cytoskeletal-membrane interactions: Between cell surface glycoconjugates and doublet microtubules of the photoreceptor connecting cilium. *J Cell Biol* 105:2973–2987.
- Hunter DG, Fishman GA, Metha RS, Kretzer FL. 1986. Abnormal sperm and photoreceptor axonemes in Usher's Syndrome. *Arch Ophthalmol* 104:385–389.
- Isenberg G, Niggli V. 1998. Interaction of cytoskeletal proteins with membrane lipids. *Int Rev Cytol* 178:73–125.
- Lessard JL. 1988. Two monoclonal antibodies to actin: one muscle selective and one generally reactive. *Cell Motil Cytoskeleton* 10:349–362.
- Liu X, Udovichenko IP, Brown SD, Steel KP, Williams DS. 1999. Myosin VIIa participates in opsin transport through the photoreceptor cilium. *J Neurosci* 19:6267–6274.
- Liu XR, Vansant G, Udovichenko IP, Wolfrum U, Williams DS. 1997. Myosin VIIa, the product of the Usher 1B syndrome gene, is concentrated in the connecting cilia of photoreceptor cells. *Cell Motil Cytoskeleton* 37:240–252.

- Marszalek JR, Liu X, Roberts E, Chui D, Marth J, Williams DS, Goldstein LSB. 1998. Tissue specific deletion of KIF3A from photoreceptors results in their degeneration. *Mol Biol Cell* 9:131a.
- Matsumoto B, Hale IL. 1993. Preparation of retinas for studying photoreceptors with confocal microscopy. In: Hargrave PA, editor. *Photoreceptor cells*. San Diego, CA: Academic Press. p 54–71.
- Matsusaka T. 1974. Membrane particles of the connecting cilium. *J Ultrastruct Res* 48:305–312.
- Mburu P, Liu XZ, Walsh J, Saw D, Jamie M, Cope TV, Gibson F, Kendrick-Jones J, Steel KP, Brown SDM. 1997. Mutation analysis of the mouse myosin VIIA deafness gene. *Genes Funct* 1:191–203.
- Miyaguchi K, Hashimoto PH. 1992. Evidence for the transport of opsin in the connecting cilium and basal rod outer segment in rat retina—rapid-freeze, deep-etch and horseradish peroxidase labelling studies. *J Neurocytol* 21:449–457.
- Muresan V, Bendala-Tufanisco E, Hollander BA, Besharse JC. 1997. Evidence for kinesin-related proteins associated with the axoneme of retinal photoreceptors. *Exp Eye Res* 64:895–903.
- Nir I, Papermaster DS. 1983. Differential distribution of opsin in the plasma membrane of frog photoreceptors: an immunocytochemical study. *Invest Ophthalmol Visual Sci* 24:868–878.
- Nir I, Papermaster DS. 1986. Immunocytochemical localization of opsin in the inner segment and ciliary plasma membrane of photoreceptors in retinas of rds mutant mice. *Invest Ophthalmol Visual Sci* 27:836–840.
- Nir I, Cohen D, Papermaster DS. 1984. Immunocytochemical localization of opsin in the cell membrane of developing rat retinal photoreceptors. *J Cell Biol* 98:1788–1795.
- Nir I, Sagie G, Papermaster DS. 1987. Opsin accumulation in photoreceptor inner segment plasma membranes of dystrophic RCS rats. *Invest Ophthalmol Visual Sci* 28:62–69.
- Nir I, Agarwal N, Sagie G, Papermaster DS. 1989. Opsin distribution and synthesis in degenerating photoreceptors of rd mutant mice. *Exp Eye Res* 49:403–421.
- Obata S, Usukura J. 1992. Morphogenesis of the photoreceptor outer segment during postnatal development in the mouse (BALB/c) retina. *Cell Tissue Res* 269:39–48.
- Pagh-Roehl K, Burnside B. 1995. Preparation of teleost rod inner and outer segments. In: Dentler W, Witman G, editors. *Cilia and flagella*. San Diego, CA: Academic Press. p 89–92.
- Papermaster DS, Schneider BG. 1982. Biosynthesis and morphogenesis of outer segment membranes in vertebrate photoreceptor cells. In: McDevitt DS, editor. *Cell biology of the eye*. San Diego, CA: Academic Press. p 475–531.
- Papermaster DS, Schneider BG, Besharse JC. 1985. Vesicular transport of newly synthesized opsin from the Golgi apparatus toward the rod outer segment. *Invest Ophthalmol Visual Sci* 26:1386–1404.
- Papermaster DS, Schneider BG, DeFoe D, Besharse JC. 1986. Biosynthesis and vectorial transport of opsin on vesicles in retinal rod photoreceptors. *J Histochem Cytochem* 34:5–16.
- Peters KR, Palade GE, Schneider BG, Papermaster DS. 1983. Fine structure of a periciliary ridge complex of frog retinal rod cells revealed by ultrahigh resolution scanning electron microscopy. *J Cell Biol* 96:265–276.
- Piperno G, Luck DJL. 1979. An actin-like protein is a component of axonemes from *Chlamydomonas*. *J Biol Chem* 254:2187–2190.
- Richardson GP, Forge A, Kros CJ, Fleming J, Brown SDM, Steel KP. 1997. Myosin VIIA is required for aminoglycoside accumulation in cochlear hair cells. *J Neurosci* 17:9506–9519.
- Richardson TM. 1969. Cytoplasmic and ciliary connections between the inner and outer segments of mammalian visual receptors. *Vision Res* 9:727–731.
- Roof DJ, Heuser JE. 1982. Surface of rod photoreceptor disk membrane components. *J Cell Biol* 95:487–500.
- Roof DJ, Adamian M, Hayes A. 1994. Rhodopsin accumulation at abnormal sites in retinas of mice with a human P23H rhodopsin transgene. *Invest Ophthalmol Visual Sci* 35:4049–4062.
- Röhlich P. 1975. The sensory cilium of retinal rods is analogous to the transitional zone of motile cilia. *Cell Tissue Res* 161:421–430.
- Steinberg RH, Fisher SK, Anderson DH. 1980. Disc morphogenesis in vertebrate photoreceptors. *J Comp Neurol* 190:501–518.
- Sung CH, Makino C, Baylor D, Nathans J. 1994. A rhodopsin gene mutation responsible for autosomal dominant retinitis pigmentosa results in a protein that is defective in localization to the photoreceptor outer segment. *J Neurosci* 14:5818–5833.
- Tai AW, Chuang JZ, Bode C, Wolfrum U, Sung CH. 1999. Rhodopsin's carboxy-terminal cytoplasmic tail acts as a membrane receptor for cytoplasmic dynein by binding to dynein light chain Tctex-1. *Cell* 97:877–887.
- Usukura J, Obata S. 1995. Morphogenesis of photoreceptor outer segments in retinal development. *Prog Retin Eye Res* 15:113–125.
- Weil D, Levy G, Sahly I, Levia-Cobas F, Blanchard S, El-Amraoui A, Crozet F, Philippe H, Abitbol M, Petit C. 1996. Human myosin VIIA responsible for the Usher 1B syndrome: a predicted membrane-associated motor protein expressed in developing sensory epithelia. *Proc Natl Acad Sci USA* 93:3232–3237.
- Whitehead JL, Wang SY, Bost UL, Hoang E, Frazer KA, Burnside B. 1999. Photoreceptor localization of the KIF3A and KIF3B subunits of the heterotrimeric microtubule motor kinesin II in vertebrate retina. *Exp Cell Res* 69:491–503.
- Williams DS, Hallett, MA, Arikawa K. 1992. Association of myosin with the connecting cilium of rod photoreceptor cells. *J Cell Sci* 103:183–190.
- Williams DS, Marszalek JR, Liu X, Roberts E, Goldstein LS. 1999. Selective cre-lox knockout of the kinesin, KIF3A, in mouse photoreceptors leads to degeneration. *Invest Ophthalmol Visual Sci* 40:3391.
- Wolenski JS, Cheney RE, Mooseker MS, Forscher P. 1995. In vitro motility of immunoadsorbed brain myosin-V using a *Limulus* acrosomal process and optical tweezer-based assay. *J Cell Sci* 108:1489–1496.
- Wolfrum U. 1991. Tropomyosin is co-localized with the actin filaments of the scolopale in insect sensilla. *Cell Tissue Res* 265:11–17.
- Wolfrum U. 1995. Centrin in the photoreceptor cells of mammalian retinae. *Cell Motil Cytoskeleton* 32:55–64.
- Wolfrum U. 1997. Cytoskeletal elements in insect sensilla. *Int J Insect Morphol Embryol* 26:191–203.
- Wolfrum U, Schmitt A. 1999. Evidence for myosin VIIa driven rhodopsin transport in the plasma membrane of the photoreceptor connecting cilium. In: Hollyfield JG, Andersson RE, LaVail M, editors. *Retinal degeneration diseases and experimental therapy*. New York: Plenum Press. p 3–14.
- Young RW. 1967. The renewal of photoreceptor cell outer segments. *J Cell Biol* 33:61–72.
- Young RW. 1968. Passage of newly formed protein through the connecting cilium of retinal rods in the frog. *J Ultrastruct Res* 23:462–473.
- Young RW. 1976. Visual cells and the concept renewal. *Invest Ophthalmol* 15:700–725.
- Young RW, Droz B. 1968. The renewal of protein in retinal rods and cones. *J Cell Biol* 39:169–184.